Dartmouth College
Dartmouth Digital Commons

Open Dartmouth: Published works by Dartmouth faculty

Faculty Work

8-10-2007

Mixing and Homogenization in the Early Solar System: Clues from Sr, Ba, Nd, and Sm Isotopes in Meteorites

Rasmus Andreasen
Dartmouth College

Mukul Sharma
Dartmouth College

Follow this and additional works at: https://digitalcommons.dartmouth.edu/facoa

 Part of the The Sun and the Solar System Commons

Dartmouth Digital Commons Citation

Andreasen, Rasmus and Sharma, Mukul, "Mixing and Homogenization in the Early Solar System: Clues from Sr, Ba, Nd, and Sm Isotopes in Meteorites" (2007). *Open Dartmouth: Published works by Dartmouth faculty*. 2250.
https://digitalcommons.dartmouth.edu/facoa/2250

This Article is brought to you for free and open access by the Faculty Work at Dartmouth Digital Commons. It has been accepted for inclusion in Open Dartmouth: Published works by Dartmouth faculty by an authorized administrator of Dartmouth Digital Commons. For more information, please contact dartmouthdigitalcommons@groups.dartmouth.edu.

The Astrophysical Journal, 665:874–883, 2007 August 10
© 2007. The American Astronomical Society. All rights reserved. Printed in U.S.A.

MIXING AND HOMOGENIZATION IN THE EARLY SOLAR SYSTEM: CLUES FROM Sr, Ba, Nd, AND Sm ISOTOPES IN METEORITES

Rasmus Andreasen and Mukul Sharma
Department of Earth Sciences, Dartmouth College, 6105 Sherman Fairchild Hall, Hanover, NH 03755;
rasmus.andreasen.adv07@alum.dartmouth.edu, mukul.sharma@dartmouth.edu
Received 2006 December 1; accepted 2007 April 7

ABSTRACT

High-precision barium isotopic compositions of large samples of an ordinary chondrite and a eucrite are identical to the terrestrial values. In contrast, the carbonaceous chondrites reveal excesses in ^{135}Ba and ^{137}Ba of around +39 and +22 parts per million (ppm), respectively; no anomalies are resolvable in ^{130,132,138}Ba. High-precision Sr isotopic compositions of all meteorites are identical within error. The data are consistent with the carbonaceous chondrites having an excess in the *r*-process ^{135,137}Ba with respect to Earth, eucrite parent bodies, and ordinary chondrites. The carbonaceous chondrites, however, display no variation in the *r*- and *s*-process Sm and Nd isotopes, suggesting that the *r*-process sources of Ba and the lanthanides were decoupled. The homogeneity of Ba and Sm isotopes in the Earth, eucrite parent body, and ordinary chondrite indicates that the solar nebula that fed planetesimals between ~1 and ~2.4 AU was well mixed with respect to these isotopes. It was heterogeneous beyond ~2.7 AU where carbonaceous chondrite parent bodies formed. These observations also indicate that the best estimate of the Nd isotopic composition of the Earth is obtained from ordinary chondrites and not from carbonaceous chondrites, as is normally assumed. Since the terrestrial upper mantle shows a ^{142}Nd anomaly of +18 ± 8 ppm with respect to the ordinary chondrites, this is further evidence that the upper mantle retains a memory of early Earth differentiation and sequestration of a reservoir with an average Sm/Nd ratio lower than that of chondrites.

Subject headings: Earth — meteors, meteoroids — nuclear reactions, nucleosynthesis, abundances — solar system: formation — supernovae: general

1. INTRODUCTION

The material in the solar system is a mixture of debris from widely different nucleosynthetic sources. It has long been established that calcium-aluminum–rich inclusions (CAIs) found in meteorites have very variable isotopic composition of heavy elements such as Ca, Ti, Ba, Nd, Sm (e.g., Lee et al. 1978; Lugmair et al. 1978; McCulloch & Wasserburg 1978a, 1978b; Niederer et al. 1981; Papanastassiou & Wasserburg 1978; Wasserburg et al. 1980; for a recent summary see Birck 2004) due to somewhat different blends of the original components. These inclusions are typical macroscopic samples that have been chemically processed within the solar system but are not isotopically representative of the "bulk" solar system. Furthermore, microscopic/submicroscopic interstellar dust grains formed as circumstellar condensates around asymptotic giant branch (AGB) stars or during explosions of supernovae have been discovered in a wide variety of different meteorites (e.g., Huss 1990; Lodders & Amari 2005; Nittler 2003). These have very large shifts in isotopic composition relative to the solar values (see reviews by Zinner [1998] and Meyer & Zinner [2006]). The preservation of these different materials in bulk meteorites may therefore reflect the degree and scale of heterogeneity within the early solar system when planetary bodies formed. The differences in isotopic composition of bulk meteorite samples may reflect variations in the mixing ratio of the various components in different "planetary" materials. It would then follow that models of planetary evolution that are based on the small shifts in isotopic ratios due to radioactive decay are strongly dependent on the initial isotopic state and a "bulk solar" value that cannot be properly assumed. For example, a key issue to understand the evolution of early Earth has been whether the available samples of meteorites accurately reflect the Nd isotopic composition of the bulk Earth.

That the terrestrial upper mantle displays a ^{142}Nd anomaly of around +20μ (=1 ppm) with respect to chondrites and basaltic eucrites has been taken as evidence for global terrestrial differentiation leading to an upper mantle with high Sm/Nd ratio when short-lived ^{146}Sm (^{146}Sm→^{142}Nd; $t_{1/2} = 103$ Myr) was alive (Boyet & Carlson 2005). This inference calls for sequestration of a low Sm/Nd reservoir deep in the Earth and is supported by the finding that the bulk Moon Nd isotopic composition is chondritic (Rankenburg et al. 2006). However, as ^{142}Nd is an *s*-process nuclide with a small *p*-process contribution and the rest of the Nd isotopes have variable *r*-process contributions, the possibility remains that the chondrites and the eucrite parent bodies have an *r*-process excess (or *p*- or *s*-process deficit) relative to Earth. This question was investigated by Andreasen & Sharma (2006), who discovered that carbonaceous chondrites have a deficit of about 100μ in the *p*-process ^{144}Sm (and ^{146}Sm), which is consistent with and likely the cause of the bimodality in the ^{142}Nd values for carbonaceous versus ordinary chondrites. However, the uniform ^{148}Sm/^{154}Sm and ^{145}Nd/^{144}Nd ratios in ordinary and carbonaceous chondrites, a eucrite, and Earth indicate a solar nebula with a rather uniform *r*/*s* ratio. This strongly supports early differentiation as the cause for the elevated ^{142}Nd values seen in terrestrial samples relative to other planetary bodies. A different approach to the same question was taken by Ranen & Jacobsen (2006), who found anomalies in ^{137}Ba and ^{138}Ba in both carbonaceous and ordinary chondrites and attributed them to excesses in *r*-process or neutron burst material in the meteorites relative to Earth. Such an excess would produce a negative ^{142}Nd anomaly in the chondrites. The Ba isotope data thus imply different initial Nd isotopic states for the chondrites and Earth and do not require an early terrestrial silicate differentiation event. However, a uniform *r*/*s* ratio for the solar nebula as inferred from Sm and Nd isotopes and an *r*-excess inferred from Ba isotopes may alternatively imply different sources of *r*-process Ba and

lanthanides. Moreover, as the chondrites contain variable proportions of chondrules, CAIs, and presolar SiC grains that display δ to ε unit (δ = parts in 10^3 or permil; ε = parts in 10^4) variations in *s*-, *r*-, and *p*-process isotopes (Lugmair et al. 1983; McCulloch & Wasserburg 1978a; Ott & Begemann 1990; Papanastassiou & Wasserburg 1978; Patchett 1980; Prombo et al. 1993; Zinner et al. 1991) a related question is whether the small isotope anomalies in macroscopic samples reflect nucleosynthetic variations or incomplete dissolution of presolar grains or CAIs.

We have investigated these issues further by obtaining Ba and Sr isotopic compositions of the same sample aliquots for which Nd and Sm isotope analyses have been already reported (Andreasen & Sharma 2006). This was done to (1) minimize the issue of sample inhomogeneity and get a complete picture of the variations in nucleosynthetic components for different elements and (2) evaluate if the observed variations could be due to incomplete dissolution of the samples. Barium is well suited for studying nucleosynthetic variations (Eugster et al. 1969; McCulloch & Wasserburg 1978a; Ranen & Jacobsen 2006), the low-abundance ^{130}Ba and ^{132}Ba are *p*-only nuclides; ^{134}Ba and ^{136}Ba are *s*-only nuclides shielded from *r*-contribution by ^{134}Xe and ^{136}Xe and with a constant ratio are thus ideal to use for fractionation correction. ^{135}Ba, ^{137}Ba, and ^{138}Ba are mixtures of *s*- and *r*-process. There is a possibility that ^{135}Ba variations are due to the decay of short-lived ^{135}Cs ($^{135}\text{Cs} \rightarrow {}^{135}\text{Ba}$, $t_{1/2} = 2.3$ Myr) (Hidaka et al. 2001; McCulloch & Wasserburg 1978a; Nichols et al. 2002). Comparing any ^{135}Ba anomalies with ^{137}Ba and ^{138}Ba should make it possible to identify the cause of the anomaly. Decomposition of strontium isotopic composition into different nucleosynthetic components is not straightforward (Papanastassiou & Wasserburg 1978; Wasserburg et al. 1980). Sr has four isotopes: ^{84}Sr is a *p*-only nuclide, ^{86}Sr and ^{87}Sr are *s*-only nuclides, shielded by ^{86}Kr and ^{87}Rb, and ^{88}Sr is predominantly *s*-process with some *r*-process contribution. As ^{87}Rb is a long-lived radioactive nuclide decaying to ^{87}Sr ($t_{1/2} = 48.8$ Gyr), large variations in ^{87}Sr due to different Rb/Sr ratios result, making ^{87}Sr unsuitable to investigate nucleosynthetic variations. This leaves a *p*-only, an *s*-only, and an $s + r$ nuclide, yielding only one variable when the data are fractionation corrected. Furthermore, when interpreting Sr isotope data it is important to recognize that isotope anomalies may be introduced by incorrect fractionation correction (see detailed discussion in Wasserburg et al. 1980).

In this paper, we show that (1) the Ba, Nd, and Sm isotopic compositions of the terrestrial samples, a eucrite (Juvinas), and an ordinary chondrite (St. Severin, LL6) are identical to each other and distinct from that of the carbonaceous chondrites (Allende, CV3; and Murchison, CM2) and (2) the isotope effects in the latter do not to result from incomplete dissolution of the constituent phases. We also show that Sr isotopic composition of bulk samples of all meteorites is uniform and identical to the terrestrial composition. In § 2 we present details of experimental techniques, and in § 3 we present results of high-precision measurements. In § 4 we discuss the observed isotopic variations in the context of (1) mixing of nucleosynthetic components in the solar nebula, (2) potential decoupling of the sources of *r*-process Ba from those of the lanthanides, and (3) implications toward evolution of early Earth, and in § 5 we summarize our conclusions. In the Appendix we discuss the possibility of an analytical problem with the recently published results (Ranen & Jacobsen 2006) on high-precision Ba isotope measurements in chondrites.

2. ANALYTICAL METHODS

High-precision Sr and Ba isotopic compositions were determined on macroscopic 0.5 to 1 g homogenized samples (0.5 g for the eucrite, 1 g for the chondrites), which are taken to be representative of the meteorite. The data were obtained on the same sample aliquots as used for high-precision Nd and Sm isotope analyses (Andreasen & Sharma 2006). See Andreasen & Sharma (2006) for details of sample processing. Briefly, rock powder was dissolved in a combination of HF, $HClO_4$, and HNO_3 at 150°C and 20 bar for 24 hr using a PicoTrace dissolution unit. The samples were dried at 120°C for 4 hr, then at 135°C for 4 hr and finally at 220°C for 48 hr in an atmosphere of dry N_2. The heating ramp ensures subboiling evaporation of the acid mixture, whose composition changes with time; the last heating step is necessary to completely remove $HClO_4$. The residues were dissolved in 6 M HCl, then dried and redissolved in 1.5 M HCl. For the carbonaceous chondrites the resulting solution contained a very small residue. Although, our dissolution procedure is different from that employed by Pilger et al. (1995) to dissolve SiC grains, it is possibly more aggressive.

The Sr and Ba fractions were collected using cation exchange columns. The fractions were further purified using small Teflon columns (volume 100 μl) filled with Eichrom Sr-spec resin. The purification step, following the guidelines of Chabaux et al. (1994), ensured complete separation of Rb from the Sr fraction and La and Ce from the Ba fraction.

Approximately 500 ng Sr or Ba were loaded on a rhenium side filament in 1 μl of 2.5 M HCl and 1 μl of 0.2 M H_3PO_4. Highly stable and intense ion beams were obtained using the double filament configuration on the Dartmouth Triton thermal ionization mass spectrometer. We measured the Sr isotopic composition in static mode after obtaining an ^{88}Sr intensity of 1×10^{-10} A. A symmetric Faraday detector setup with ^{86}Sr in the center cup, ^{84}Sr and ^{85}Rb on the low-mass side, and ^{87}Sr and ^{88}Sr on the high-mass side was used. The isobaric interference of ^{87}Rb on ^{87}Sr estimated from the measured higher intensity of ^{85}Rb was less than 1 ppm for all samples. The data were collected for 90 blocks with each block containing 15 ratios that, in turn, were obtained by integrating the ion beams for about 8 s. Baselines were measured for 30 s at the beginning of every block and the amplifier connections rotated after each block.

All seven isotopes of barium were measured in static mode. Possible isobaric interferences of ^{138}La, ^{136}Ce, and ^{138}Ce were determined before and after each analysis using ^{139}La and ^{140}Ce. The La and Ce interferences were for all samples and standards found to be less than 0.1 ppm, and no interference correction was applied. For the Ba analyses a ^{138}Ba intensity of $\sim 2 \times 10^{-10}$ A was achieved for 4 hr or more; data were collected for 70 blocks with each block comprising 20 ratios. Each ratio was obtained after integrating the ion beam for about 8 s. Baselines were measured for 30 s in the beginning of every block, and the amplifier connections rotated after each block.

3. RESULTS

The Sr and Ba isotopic compositions for the chondrites and terrestrial standards are given in Table 1 and presented in Figure 1. If the *p*-process yields follow a scaling law (Hayakawa et al. 2005), we expect ~100 ppm deficits in the *p*-nuclides ^{84}Sr, ^{130}Ba, and ^{132}Ba in carbonaceous chondrites on the basis of the observed and inferred deficits in ^{144}Sm and ^{146}Sm, respectively (Andreasen & Sharma 2006). There is, however, no resolvable deficit in ^{84}Sr in Murchison and Allende. If anything there appears to be a small but not quite resolvable positive ^{84}Sr anomaly in the carbonaceous chondrites (Fig. 1). It is evident that the $^{84}\text{Sr}/^{86}\text{Sr}$ ratios in the carbonaceous chondrites are indistinguishable at a level of ± 34 ppm (2 σ) from that of eucrite (Juvinas), ordinary chondrite (St. Severin), and terrestrial mantle. Since the $^{84}\text{Sr}/^{86}\text{Sr}$ ratio

TABLE 1
STRONTIUM ISOTOPIC COMPOSITION

Sample	^{88}Sr Average Current (pA)	Percent F	^{84}Sr/^{86}Sr[a]	^{87}Sr/^{86}Sr[a]	^{87}Sr/^{86}Sr[b]	^{88}Sr/^{86}Sr[b]	^{86}Sr/^{88}Sr[c]
NBS SRM-987 RA-21	162.1	−0.30	0.0564935(6)	0.710271(2)	0.710269(5)	8.37514(9)	0.1194005(7)
NBS SRM-987 RA-22	78.2	−0.14	0.0564948(9)	0.710256(2)	0.710260(6)	8.37533(13)	0.1193992(10)
NBS SRM-987 RA-23	75.4	−0.42	0.0564947(11)	0.710273(3)	0.710276(8)	8.37531(16)	0.1193993(11)
NBS SRM-987 RA-24	83.5	−0.16	0.0564940(9)	0.710254(2)	0.710254(6)	8.37521(13)	0.1194000(9)
NBS SRM-987 RA-25	100.7	−0.39	0.0564941(7)	0.710281(2)	0.710282(5)	8.37522(10)	0.1193999(8)
NBS SRM-987 RA-26	86.1	−0.18	0.0564940(9)	0.710256(2)	0.710258(6)	8.37521(13)	0.1194000(9)
NBS SRM-987 RA-27	94.3	−0.37	0.0564948(8)	0.710276(2)	0.710281(5)	8.37533(11)	0.1193991(8)
NBS SRM-987 RA-28	121.1	−0.25	0.0564942(6)	0.710257(2)	0.710258(4)	8.37524(9)	0.1193998(7)
NBS SRM-987 RA-30	106.2	−0.44	0.0564924(7)	0.710270(2)	0.710260(5)	8.37498(10)	0.1194016(7)
NBS SRM-987 RA-31	85.6	−0.48	0.0564925(8)	0.710263(2)	0.710253(6)	8.37499(12)	0.1194016(9)
NBS SRM-987 RA-32	97.7	−0.29	0.0564919(8)	0.710262(2)	0.710250(5)	8.37491(11)	0.1194022(8)
NBS SRM-987 RA-33	101.1	−0.28	0.0564934(7)	0.710268(2)	0.710260(5)	8.37513(11)	0.1194006(8)
Average (n = 12)			0.0564937(19)	0.710265(18)	0.710263(22)	8.37517(28)	0.1194003(20)
2 σ uncertainty (ppm)			34	25	31	34	17
BCR-2 Sr-I	88.7	−0.31	0.0564928(9)	0.705020(2)	0.705014(6)	8.37504(12)	0.1194012(9)
BCR-2 Sr-II	87.2	−0.22	0.0564926(8)	0.705018(2)	0.705012(5)	8.37500(12)	0.1194015(8)
BCR-2 Sr-III	82.2	−0.26	0.0564951(8)	0.705018(2)	0.705025(6)	8.37538(12)	0.1193988(9)
BCR-2 Sr-IV	101.8	−0.32	0.0564915(7)	0.705023(2)	0.705007(5)	8.37484(10)	0.1194026(8)
BCR-2 Sr-V	95.4	−0.32	0.0564934(8)	0.705021(2)	0.705019(5)	8.37512(11)	0.1194006(8)
BCR-2 Sr-VI	117.1	−0.24	0.0564928(7)	0.705024(2)	0.705018(5)	8.37504(10)	0.1194012(7)
BCR-2 Sr-VII	126.2	−0.04	0.0564913(8)	0.705024(2)	0.705006(6)	8.37481(12)	0.1194029(9)
Average (n = 7) and 2 σ uncertainty			0.0564928(26)	0.705021(5)	0.705014(13)	8.37503(37)	0.1194013(27)
Deviation from Sr-A (ppm)			−16 ± 46	−7383 ± 7	−7390 ± 20	−16 ± 45	8 ± 23
Allende CS	103.0	−0.10	0.0564974(12)	0.712213(3)	0.712234(9)	8.37570(18)	0.1193972(15)
Allende	92.9	−0.30	0.0564951(5)	0.712225(1)	0.712231(4)	8.37538(7)	0.1193988(5)
Allende*	150.4	−0.45	0.0564969(5)	0.712231(2)	0.712247(4)	8.37563(8)	0.1193970(6)
Average (n = 3) and 2 σ uncertainty			0.0564965(23)	0.712223(18)	0.712237(18)	8.37557(34)	0.1193977(20)
Deviation from Sr-A (ppm)			49 ± 42	2756 ± 26	2779 ± 25	48 ± 41	−22 ± 17
Murchison CS	96.0	−0.26	0.0564967(7)	0.728529(2)	0.728546(5)	8.37561(11)	0.1193972(8)
Murchison	91.7	−0.30	0.0564965(8)	0.728533(2)	0.728550(6)	8.37557(11)	0.1193974(8)
Murchison*	126.0	0.02	0.0564941(5)	0.728485(1)	0.728486(4)	8.37522(7)	0.1193999(5)
Average (n = 3) and 2 σ uncertainty			0.0564959(29)	0.728515(54)	0.728527(72)	8.37548(42)	0.1193981(31)
Deviation from Sr-A (ppm)			37 ± 52	25695 ± 74	25714 ± 99	36 ± 51	−18 ± 26
Juvinas CS	87.9	−0.14	0.0564941(8)	0.699434(2)	0.699434(6)	8.37523(12)	0.1193999(9)
Juvinas	100.1	−0.42	0.0564927(7)	0.699430(2)	0.699423(5)	8.37503(10)	0.1194013(7)
Juvinas	103.9	−0.43	0.0564936(7)	0.699448(2)	0.699443(5)	8.37515(10)	0.1194004(7)
Juvinas*	135.1	−0.53	0.0564936(6)	0.699435(2)	0.699432(4)	8.37515(9)	0.1194004(6)
Average (n = 4) and 2 σ uncertainty			0.0564935(12)	0.699437(15)	0.699433(17)	8.37514(17)	0.1194005(12)
Deviation from Sr-A (ppm)			−3 ± 21	−15246 ± 21	−15249 ± 24	−3 ± 20	2 ± 10
Saint-Severin CS	93.6	−0.20	0.0564940(8)	0.712763(2)	0.712763(5)	8.37521(11)	0.1194000(8)
Saint-Severin	108.5	−0.45	0.0564929(7)	0.712776(2)	0.712772(5)	8.37505(10)	0.1194011(7)
Saint-Severin*	177.9	−0.38	0.0564927(5)	0.712774(2)	0.712766(3)	8.37502(7)	0.1194014(5)
Average (n = 3) and 2 σ uncertainty			0.0564932(14)	0.712771(14)	0.712767(9)	8.37509(21)	0.1194008(15)
Deviation from Sr-A (ppm)			−9 ± 25	3528 ± 19	3525 ± 13	−9 ± 25	4 ± 12

NOTES.—Sr isotopic composition measured as Sr^+ ions by TIMS in a 5 Faraday cup static measurement setup with ^{86}Sr in the center cup. ^{87}Sr/^{86}Sr ratios are corrected for isobaric interference of ^{87}Rb, the interference correction is trivial and less than 1 ppm in all cases. "CS" denotes sample fraction spiked for Sm/Nd concentration measurements in Andreasen & Sharma (2006); asterisks denote different dissolution from same batch of powdered sample. The exponential law (Russell et al. 1978) was used to make mass fractionation corrections.

[a] Fractionation corrected to ^{88}Sr/^{86}Sr = 8.375209.

[b] Fractionation corrected to ^{84}Sr/^{86}Sr = 0.056494.

[c] Fractionation corrected to ^{84}Sr/^{88}Sr = 0.0067495.

is obtained after correcting for mass fractionation in the ion source of the mass spectrometer using an assumed ^{88}Sr/^{86}Sr ratio (Table 1), the results point to a rather homogeneous distribution of Sr isotopes in the parent bodies of the meteorites and on Earth. Furthermore, it is worth noting that the Sr isotopic ratios in the carbonaceous chondrites are unaffected by the presence of large and variable amounts of refractory CAIs and acid-resistant SiC grains displaying large variations in ^{84}Sr (Papanastassiou & Wasserburg 1978; Patchett 1980; Podosek et al. 2004). The simplest explanation of this observation is that the matrices of the carbonaceous chondrites dominate their Sr isotopic composition.

In order to assess potential p-process deficits in ^{130}Ba and ^{132}Ba in carbonaceous chondrites and to reproduce the neutron burst excesses in ^{137}Ba and ^{138}Ba in carbonaceous and ordinary chondrites as observed by Ranen & Jacobsen (2006), data were corrected for mass fractionation using ^{134}Ba and ^{136}Ba, which are both s-process nuclides. The external reproducibilities of the ^{130}Ba/^{136}Ba and ^{132}Ba/^{136}Ba ratios are 55 ppm (2 σ) and 77 ppm (2 σ), respectively (Table 2). They are not sufficient to resolve

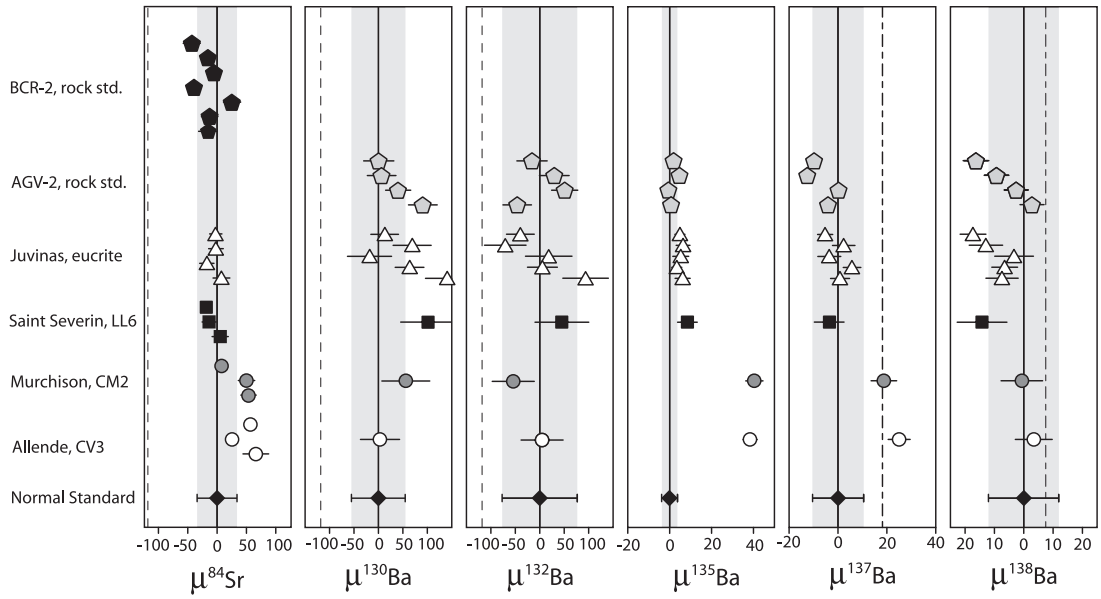

FIG. 1.—Strontium and barium isotopic composition variations for meteorites and terrestrial rocks in μ units (ppm) from normal standards, NIST SRM 987 (NIST) for Sr and VHG PBAN (VHG laboratories) for Ba. The dashed lines in ^{84}Sr, ^{130}Ba, and ^{132}Ba indicate the expected *p*-process anomaly in carbonaceous chondrites based on Sm. The dashed lines in ^{137}Ba and ^{138}Ba indicate the expected anomaly for the carbonaceous chondrites if the ^{135}Ba anomaly is due to *r*-process excess. The strontium isotopic composition is fractionation corrected using the ^{88}Sr/^{86}Sr ratio, barium using the ^{134}Ba/^{136}Ba ratio. Both Sr and Ba are corrected using the exponential law.

TABLE 2
BARIUM ISOTOPIC COMPOSITION

Sample	^{138}Ba Average Current (pA)	Percent *F*	^{130}Ba/^{136}Ba	^{132}Ba/^{136}Ba	^{135}Ba/^{136}Ba	^{137}Ba/^{136}Ba	^{138}Ba/^{136}Ba
VHG Ba RA-1	207.6	−0.18	0.0134780(3)	0.0128977(3)	0.839250(2)	1.429120(4)	9.13032(4)
VHG Ba RA-2	205.3	−0.23	0.0134775(4)	0.0128979(3)	0.839249(2)	1.429111(4)	9.13036(4)
VHG Ba RA-3	177.4	−0.22	0.0134775(4)	0.0128979(4)	0.839249(2)	1.429121(4)	9.13034(4)
VHG Ba RA-4	193.6	−0.20	0.0134784(4)	0.0128977(4)	0.839252(2)	1.429116(4)	9.13030(4)
VHG Ba RA-5	160.9	−0.21	0.0134772(4)	0.0128976(4)	0.839248(2)	1.429130(4)	9.13037(4)
VHG Ba RA-6	240.6	−0.20	0.0134780(3)	0.0128976(3)	0.839253(2)	1.429119(4)	9.13033(3)
VHG Ba RA-7	198.8	−0.18	0.0134781(4)	0.0128968(3)	0.839250(2)	1.429122(4)	9.13030(4)
VHG Ba RA-8	205.1	−0.20	0.0134780(3)	0.0128971(3)	0.839248(2)	1.429127(4)	9.13031(3)
VHG Ba RA-9	170.4	−0.22	0.0134783(4)	0.0128967(4)	0.839250(2)	1.429122(4)	9.13027(4)
VHG Ba RA-10	202.3	−0.17	0.0134782(3)	0.0128982(3)	0.839250(2)	1.429111(4)	9.13021(4)
VHG Ba RA-11	212.1	−0.18	0.0134779(3)	0.0128980(3)	0.839252(2)	1.429103(4)	9.13019(3)
Average (n = 12) and 2 σ uncertainty			0.0134779(7)	0.0128976(10)	0.839250(3)	1.429118(15)	9.13030(10)
2 σ (ppm)			55	77	4	10	12
AGV-2 Ba-II	178.4	−0.09	0.0134791(4)	0.0128970(4)	0.839251(2)	1.429113(4)	9.13032(4)
AGV-2 Ba-III	200.9	−0.06	0.0134785(3)	0.0128982(3)	0.839250(2)	1.429118(4)	9.13027(4)
AGV-2 Ba-IV	169.3	−0.12	0.0134780(4)	0.0128980(4)	0.839254(2)	1.429100(4)	9.13021(4)
AGV-2 Ba-V	162.6	−0.21	0.0134779(4)	0.0128974(4)	0.839252(2)	1.429104(4)	9.13015(4)
Average (n = 4) and 2 σ uncertainty			0.0134784(11)	0.0128976(11)	0.839252(4)	1.429109(16)	9.13024(15)
Deviation from VHG-Ba (ppm)			34 ± 83	4 ± 88	2 ± 5	−7 ± 11	−6 ± 17
Juvinas Ba-I	111.6	−0.15	0.0134798(6)	0.0128988(6)	0.839255(3)	1.429119(6)	9.13023(5)
Juvinas Ba-II	167.9	−0.04	0.0134788(4)	0.0128976(4)	0.839253(2)	1.429126(4)	9.13024(4)
Juvinas* Ba-I	183.6	0.01	0.0134777(6)	0.0128978(6)	0.839255(3)	1.429114(7)	9.13027(6)
Juvinas* Ba-II	170.1	0.18	0.0134788(5)	0.0128967(5)	0.839256(3)	1.429122(6)	9.13018(5)
Juvinas* Ba-III	181.1	−0.04	0.0134781(4)	0.0128971(4)	0.839254(2)	1.429111(4)	9.13014(4)
Average (n = 5) and 2 σ uncertainty			0.0134787(15)	0.0128976(16)	0.839254(3)	1.429118(13)	9.13021(10)
Deviation from VHG-Ba (ppm)			57 ± 113	4 ± 127	5 ± 4	0 ± 9	−10 ± 11
Allende	209.5	0.04	0.0134780(5)	0.0128976(6)	0.839282(3)	1.429154(6)	9.13033(6)
Deviation from VHG-Ba (ppm)			3 ± 40	5 ± 43	38 ± 3	25 ± 5	3 ± 6
Murchison	208.6	−0.01	0.0134787(7)	0.0128969(6)	0.839284(3)	1.429145(7)	9.13029(6)
Deviation from VHG-Ba (ppm)			56 ± 49	−54 ± 43	40 ± 4	19 ± 5	0 ± 7
Saint Severin	184.8	0.02	0.0134793(8)	0.0128982(7)	0.839257(4)	1.429113(9)	9.13017(8)
Deviation from VHG-Ba (ppm)			101 ± 56	45 ± 55	8 ± 5	−3 ± 6	−14 ± 8

NOTES.—Barium isotopic composition determined as Ba^+ ions by TIMS in a 7 Faraday cup static measurement setup. Data are fractionation corrected using the exponential law and a ^{134}Ba/^{136}Ba ratio of 0.30774. Possible isobaric interferences of La and Ce were measured just before and after data collection and were at background levels for all samples and standards. Asterisks denote different dissolution from same batch of powdered sample.

the ~100 ppm negative anomalies in the *p*-isotopes expected for the carbonaceous chondrites. However, both Murchison and Allende show well-resolved and identical anomalies of $\sim+39\mu$ and $\sim+22\mu$ for ^{135}Ba and ^{137}Ba, respectively. Significantly, the ^{138}Ba/^{136}Ba ratio of the carbonaceous chondrites cannot be resolved from that of the terrestrial mantle. These results are remarkable in that anomalies of the same magnitude ($[+39 \pm 7]\mu$ in ^{135}Ba and $[+23 \pm 8]\mu$ in ^{137}Ba) have been reported for a large sample of another carbonaceous chondrite (Orgueil, CI) and another sample of Allende (Harper et al. 1992); these workers did not report any ^{138}Ba measurements. Hidaka et al. (2003) reported relatively lower precision measurements for Allende ($[+65 \pm 32]\mu$ in ^{135}Ba and $[+49 \pm 30]\mu$ in ^{137}Ba). These data are identical within error to those reported here. Intriguingly, however, these researchers also report negative anomalies for Murchison ($[-97 \pm 18]\mu$ in ^{135}Ba and $[-50 \pm 24]\mu$ in ^{137}Ba), possibly reflecting heterogeneous distribution of *s*- or *r*-process carriers within the meteorite (see below). The Ba isotopic compositions of St. Severin and Juvinas are indistinguishable from that of the terrestrial mantle. The data for Juvinas are consistent with those measured by Hidaka et al. (2003), who also found no Ba anomaly in this eucrite.

There is, however, a clear discrepancy between our results and the ^{137}Ba and ^{138}Ba anomalies recently reported for Allende and Murchison by Ranen & Jacobsen (2006), who also found ^{137}Ba and ^{138}Ba anomalies in ordinary chondrites. Since we have not analyzed an ordinary chondrite that is common with the study by Ranen & Jacobsen (2006), the discrepancy for the ordinary chondrites could be explained due to heterogeneities between their parent bodies. This explanation, however, is not valid for the carbonaceous chondrites (Allende and Murchison) and may point to the intrinsic heterogeneities of their parent bodies to be the cause of the observed inconsistency. An alternate explanation is also possible. Ranen & Jacobsen (2006) noted that the Ba isotope patterns appear to be similar to those found in rare SiC X grains in Murchison and suggested that the chondritic meteorite parent bodies accreted a small (<0.1%) excess of neutron burst material. If so, this signal would be expected in the rather large samples of Allende and Murchison analyzed here, which is not the case. This argument, combined with the fact that no other study (this study; Hidaka et al. 2003; Carlson et al. 2007) find excesses in ^{138}Ba leads us to suspect an analytical problem with the data reported by Ranen & Jacobsen (2006). Indeed, our modeling (in the Appendix) suggests that a mass-dependent bias could be introduced during mass fractionation correction employed by Ranen & Jacobsen (2006), potentially leading to the anomalies in ^{138}Ba. Future studies cross calibrating the same sample solutions between laboratories would be needed to resolve this important issue.

4. DISCUSSION

The observed Ba anomalies in Allende and Murchison are consistent with an *r*-process excess, where ^{135}Ba has the highest *r*-contribution, and thus show the largest anomaly, the ^{137}Ba anomaly is roughly half of the ^{135}Ba anomaly, and the ^{138}Ba anomaly is roughly one-fifth of the ^{135}Ba anomaly (Figs. 1 and 2; Arlandini et al. 1999). It is curious that a μ^{137}Ba/μ^{135}Ba ratio of ~0.5 is also observed in the sample of Murchison with negative ^{135}Ba and ^{137}Ba anomalies (Hidaka et al. 2003), which indicates that the negative anomalies possibly result from an excess of SiC grains that carry *s*-process Ba nuclides (Jennings et al. 2002; Lugaro et al. 2003; Ott & Begemann 1990; Prombo et al. 1992; Savina et al. 2003; Zinner et al. 1991) or a deficit in *r*-process carriers in the analyzed sample. In this study we used a much larger homogenized sample of Murchison (an aliquot of 1 g from 8 g powder) as opposed to that used by Hidaka et al. (an aliquot of 0.08–0.1 g from a 0.3–0.5 g powder) and assume in the following that our data better represent the bulk meteorite.

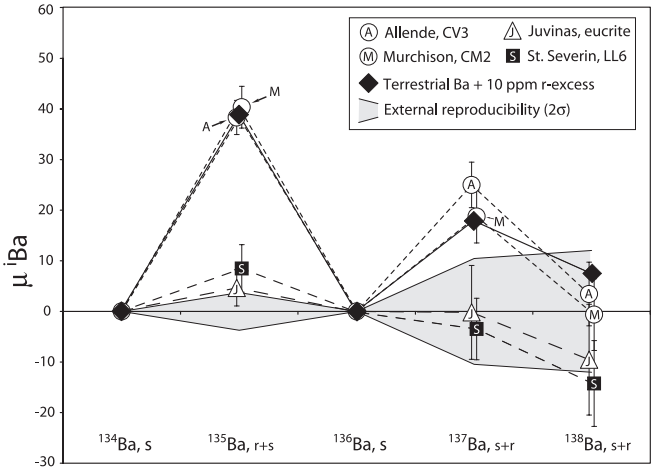

FIG. 2.—Deviations in Ba isotopic composition from that of terrestrial standard. Calculated deviation from terrestrial Ba plus 10 ppm *r*-process Ba, based on Arlandini et al. (1999), is shown as diamonds connected by a solid line. Data are fractionation-corrected using ^{134}Ba/^{136}Ba = 0.30774 (McCulloch & Wasserburg 1978a), deviations for the low-abundance ^{130}Ba and ^{132}Ba are omitted for clarity due to their lower precision.

The Ba isotope anomaly patterns for Murchison and Allende (Fig. 2) are distinctly different from those resulting from nuclear field effects (Fujii et al. 2006); in contrast to the observed patterns, nuclear field effects would result in positive anomalies of similar magnitudes in ^{135}Ba and ^{137}Ba and a negative anomaly in ^{138}Ba. Thus, the nuclear field effects are not a likely cause of the observed anomalies. However, the presence of *r*-process anomalies in Allende and Murchison and its absence in Juvinas and St. Severin is intriguing. In comparison to the carbonaceous chondrites, which were likely not heated beyond 300°C, St. Severin (LL6) was subjected to early high degrees of metamorphism (Ashworth 1980; Ashworth & Barber 1977; Chen et al. 1998; Glavin & Lugmair 2003; Leroux et al. 1996), and Juvinas (basaltic achondrite) was produced from the melting and differentiation of an asteroid (eucrite parent body; possibly 4 Vesta; Binzel & Xu 1993; Consolmagno & Drake 1977). These observations suggest that the Ba anomalies in carbonaceous chondrites could be an artifact of incomplete dissolution of acid-resistant SiC grains from AGB stars carrying the *s*-process Ba nuclides and are destroyed during high degrees of metamorphism or melting (Huss 1990; Huss & Lewis 1995).

Using the *s*-process isotopic composition from Ott & Begemann (1990) and a maximum Ba concentration of ~10 ppm in SiC (Virag et al. 1992), we find that only 14 ppm of SiC in a meteorite, if left undissolved, would produce a ^{135}Ba anomaly of $+38\mu$, a ^{137}Ba anomaly of $+21\mu$, and a ^{138}Ba anomaly of $+11\mu$, similar to the values measured for Allende and Murchison. We note, however, that Allende and Murchison have vastly different SiC abundances; they are less than 10 parts per billion (ppb) in Allende (Huss & Lewis 1995) and about 3 orders of magnitude higher in Murchison (Tizard et al. 2005). This suggests that an *s*-process deficit due to incomplete dissolution of presolar grains should result in essentially no Ba anomaly in Allende and pronounced anomalies in Murchison. Furthermore, high-precision Nd and Sm isotopic data from the same sample aliquots (Andreasen & Sharma 2006) do not show *s*-process deficits, as would likely be expected if the Ba isotopic pattern were produced from the incomplete dissolution. However, the Sm may not provide a strict test; if

the Sm/Nd ratio in SiC is as low as suggested by Yin et al. (2006), then the expected effects in Sm isotopic composition due to incomplete SiC dissolution would not be resolvable at the current level of precision. Possible explanations for the similar values observed in Allende and Murchison could be that the Ba concentration of SiC grains is too low to exert control on the bulk sample Ba isotopic composition, or that the high P-T HF-HNO_3-$HClO_4$ dissolution protocol used in this study dissolved all SiC. Regardless, it appears that the presolar SiC grains carrying *s*-process Ba are not responsible for the anomalies observed in large homogenous samples of Murchison and Allende.

Lewis et al. (1991) found that nanodiamonds from Allende hosting isotopically anomalous Xe-HL possess *r*-process Ba nuclides ($\varepsilon^{135}\mathrm{Ba} = 12.2 \pm 3.8$ and $\varepsilon^{137}\mathrm{Ba} = 6.0 \pm 1.5$). Low abundances of nanodiamonds in Allende and Murchison ($\sim$600 ppm) combined with their low Ba content (14 ng g^{-1}) indicate that preferential incorporation of nanodiamonds cannot provide the *r*-process Ba excess in the carbonaceous chondrites. Among other acid-resistant phases observed in carbonaceous chondrites, only graphite is abundant enough (Nittler 2003) to possibly exert some control on the bulk sample Ba isotopic composition. Lewis et al. (1983) analyzed carbon-rich residues of Allende and found their Ba isotopic composition to be normal. Therefore, incomplete dissolution of carbon phases also cannot be the cause of the observed Ba anomalies. These observations suggest that rare supernovae-derived silicate phases (olivine, pyroxene, or amorphous silicate; Clayton et al. 1997; Messenger et al. 2005) may carry the *r*-process Ba and other refractory nuclei.

Since the first indication of live ^{135}Cs in the early solar system was found (McCulloch & Wasserburg 1978a), only one study has successfully found evidence for the presence of ^{135}Cs at the time of solar system formation (Hidaka et al. 2001), and one has found suggestions of variations in ^{135}Ba from ^{135}Cs decay in presolar material (Nichols et al. 2002). The challenges of using the Cs–Ba chronometer for early solar system studies are partly due to the short half-life of ^{135}Cs (2.3 Myr) and the low solar system initial $^{135}\mathrm{Cs}/^{133}\mathrm{Cs}$ ratio (Hidaka et al. 2001) and partly due to the limited fractionation between Cs and Ba in meteorites and the technical difficulties in obtaining accurate and precise Cs concentration measurements. Keeping these limitations in mind, initial $^{135}\mathrm{Cs}/^{133}\mathrm{Cs}$ and $^{135}\mathrm{Ba}/^{136}\mathrm{Ba}$ ratios at the time of formation of parent bodies of Allende and Murchison can be found, assuming that their initial $^{135}\mathrm{Ba}/^{136}\mathrm{Ba}$ ratio was constant, an assumption justified by the identical Sm and Nd isotopic compositions of these meteorites (Andreasen & Sharma 2006). According to the concentration measurements of Nakamura (1974) and Wolf et al. (2005), Murchison has a Cs/Ba ratio of 0.041 ± 3, roughly a factor of 2 higher than that of Allende (0.018 ± 2). Using the relationship

$$\left(\frac{^{135}\mathrm{Ba}}{^{136}\mathrm{Ba}}\right)_{\mathrm{Meas}} = \left(\frac{^{135}\mathrm{Ba}}{^{136}\mathrm{Ba}}\right)_{\mathrm{Init}} + \left(\frac{^{135}\mathrm{Cs}}{^{133}\mathrm{Cs}}\right)_{\mathrm{Init}} \left(\frac{^{133}\mathrm{Cs}}{^{136}\mathrm{Ba}}\right),$$

the calculated $^{135}\mathrm{Cs}/^{133}\mathrm{Cs}$ ratio at the time of formation of the carbonaceous chondrites was less than 1.7×10^{-5}. This is in agreement with the CM chondrite estimate of $(6.6 \pm 5.0) \times 10^{-5}$ (Hidaka et al. 2003) and the H chondrite estimate of $(0.2\text{–}1.3) \times 10^{-5}$ (Hidaka et al. 2001). This indicates that the carbonaceous chondrite parent bodies formed at least 7.5–10.8 Myr after the formation of Allende CAIs with $^{135}\mathrm{Cs}/^{133}\mathrm{Cs} = (4.8 \pm 0.8) \times 10^{-4}$ (Hidaka et al. 2001; McCulloch & Wasserburg 1978a).

More significantly, the initial $^{135}\mathrm{Ba}/^{136}\mathrm{Ba}$ ratio calculated for the carbonaceous chondrites (at Cs/Ba = 0) is +30 to +43μ units *higher* than that measured today for the terrestrial mantle, Juvinas, and St. Severin. This observation is intriguing as it indicates that the carbonaceous chondrites could not originate from the same Ba reservoir as the Earth, the eucrite parent body (EPB), and the LL-chondrite parent body, unless these all suffered volatile Cs loss to the same extent while ^{135}Cs was alive. In order to investigate this issue further, we regressed μ^{135}Ba against μ^{137}Ba for the available bulk carbonaceous and ordinary chondrites (this study; Hidaka et al. 2003; Harper et al. 1992). The data are positively correlated and give a statistically significant (at 95% confidence level) $\mu^{137}\mathrm{Ba}/\mu^{135}\mathrm{Ba}$ ratio of 0.52 ± 0.21 and a μ^{135}Ba intercept of 1 ± 14 ppm. The $\mu^{137}\mathrm{Ba}/\mu^{135}\mathrm{Ba}$ ratio is within error of the calculated *r*-process ratio of 0.47 (Arlandini et al. 1999). The simplest interpretation of this correlation is that the observed difference in $^{135}\mathrm{Ba}/^{136}\mathrm{Ba}$ ratio between the carbonaceous chondrites on one hand and the Earth, EPB, and LL-chondrite parent body on the other is likely the result of different degrees of incorporation of *r*-process material and not related to the decay of ^{135}Cs.

If an *r*-process excess similar to that in Ba is present in Sr for the carbonaceous chondrites, the $^{84}\mathrm{Sr}/^{86}\mathrm{Sr}$ ratio would increase by $\sim 12\mu$ due to incorrect fractionation correction, as the carbonaceous chondrites would have elevated $^{88}\mathrm{Sr}/^{86}\mathrm{Sr}$ ratios relative to terrestrial samples. This effect is not large enough to mask a *p*-process deficit in ^{84}Sr of the magnitude of that seen for Sm and Nd. The absence of measurable deficits in ^{84}Sr for the carbonaceous chondrites is therefore not due to a combination of *p*-process deficit and *r*-process excess. However, a possible *r*-process excess in Sr similar to that in Ba may be the cause of the slightly positive but not resolvable ^{84}Sr anomalies seen in the carbonaceous chondrites (Fig. 1 and Table 1).

The $^{148}\mathrm{Sm}/^{154}\mathrm{Sm}$ and $^{145}\mathrm{Nd}/^{144}\mathrm{Nd}$ isotopic ratios, which are sensitive to variations in *r*/*s* ratios, are quite uniform for ordinary chondrites, the EPB, and the Earth (Andreasen & Sharma 2006; Boyet & Carlson 2005) and suggest that *s*- and *r*-process nuclides were, on average, rather homogeneously distributed in the inner solar nebula (between 1 and 2.4 AU). This is further supported by the absence of Sr and Ba isotope anomalies in St. Severin and Juvinas with respect to the Earth. In contrast, both Allende and Murchison display deficits in *p*-process Sm and Nd isotopes (Andreasen & Sharma 2006) and excesses in *r*-process ^{135}Ba and ^{137}Ba. As the carbonaceous chondrites likely formed in the outer asteroidal belt (>2.7 AU), we infer that the *p*-, *s*-, and *r*-nuclei were heterogeneously distributed in the solar nebula, except in the region between 1 and 2.4 AU. This conclusion is consistent with a uniform distribution of *s*- and *r*-process Mo (Becker & Walker 2003a), Ru (Becker & Walker 2003b), Zr (Schönbächler et al. 2003), and Os (Brandon et al. 2006; Yokoyama et al. 2007) isotopes in the inner solar nebula. It is also consistent with recent simulations of formation of terrestrial planets that suggest extensive radial mixing of the material between 1 and 2.5 AU (Chambers 2004; O'Brien et al. 2006).

The presence of *r*-process Ba nuclide anomalies in carbonaceous chondrites and their absence in the eucrite and LL-chondrite parent bodies also indicates that (1) the Sm, Nd, and Ba isotopic composition of the EPB, LL-chondrite parent body, and bulk Earth should be identical, and (2) the source/carrier of *r*-process Ba isotopes was distinct from that of Sm and Nd isotopes. We explore these observations further by calculating enrichment factors η_s and η_r for *s*- and *r*-process dominant nuclides, respectively, in a manner similar to Mathews & Fowler (1981): $\eta_s^i \times 10^6 = \mu^i/f_s^i$ and $\eta_r^i \times 10^6 = \mu^i/f_r^i$, where μ is the measured anomaly for isotope *i* in ppm calculated with respect to the terrestrial upper mantle, f_s is the fraction of isotope *i* produced by *s*-process using the currently accepted stellar model, and f_r is the fraction of isotope *i* produced by the *r*-process calculated by subtracting

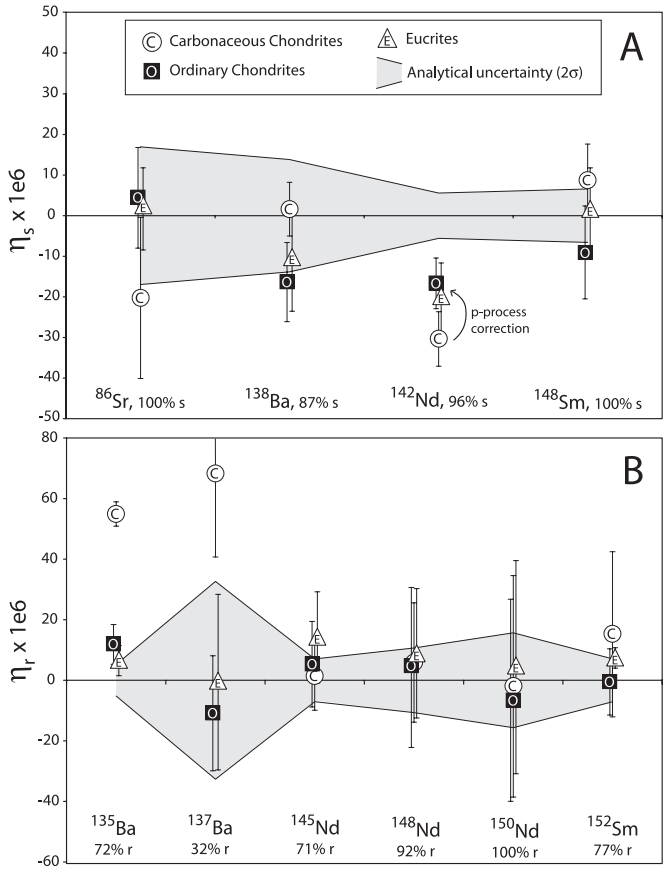

FIG. 3.—Enrichment factors for *s*-process (*a*) and *r*-process (*b*) isotopes of Sr, Ba, Nd, and Sm in meteorites, with Nd data from Boyet & Carlson (2005) and Andreasen & Sharma (2006) and Sm data from Andreasen & Sharma (2006). The enrichment factor η_s and η_r are calculated in a similar manner to Mathews & Fowler (1981) as $\eta_s^i \times 10^6 = \mu^i/f_s^i$ and $\eta_r^i \times 10^6 = \mu^i/f_r^i$, respectively, where μ is the measured anomaly for isotope i in ppm, f_s is the fraction of isotope i produced by *s*-process, and f_r is the fraction of isotope i produced by *r*-process. The nuclide fractions are taken from Arlandini et al. (1999). The error bars and shaded area represent the analytical uncertainty scaled to η and does not include uncertainties in the stellar models. ^{87}Sr and ^{143}Nd are omitted because of radiogenic in-growth; ^{149}Sm and ^{150}Sm are omitted because of thermal neutron capture effects. The arrow for carbonaceous chondrites in ^{142}Nd indicates the correction for *p*-process deficit (Andreasen & Sharma 2006).

the *s*-process contribution from the solar abundance of a given nuclide (Arlandini et al. 1999).

For the *s*-dominant nuclides, the calculated enrichment factors are about zero, except for ^{142}Nd, which is enriched in the terrestrial upper mantle (Fig. 3*a*) by $(18 \pm 8)\mu$. Andreasen & Sharma (2006) discovered that in comparison to an ordinary chondrite and a eucrite, the carbonaceous chondrites were depleted in ^{142}Nd due to differential incorporation of short-lived *p*-process ^{146}Sm. That the terrestrial upper mantle does not display any variations in *s*-nuclides (^{86}Sr, ^{138}Ba, and ^{148}Sm) other than ^{142}Nd is an indication that the latter effect may not result from preferential incorporation of *s*- (or *r*-) nuclides into the Earth. We therefore agree with Boyet & Carlson (2005), who inferred that the difference between chondritic and terrestrial upper mantle ^{142}Nd is due to differentiation of the Earth during the time when ^{146}Sm was alive. However, we note that the observed effect is quite small and more stringent tests would be needed to fully resolve the issue of early Earth differentiation.

The inference of early terrestrial silicate differentiation would be valid if ^{135}Ba/^{136}Ba, ^{137}Ba/^{136}Ba, ^{138}Ba/^{136}Ba, ^{145}Nd/^{144}Nd, ^{148}Sm/^{154}Sm, and Sm/Nd ratios for all large planetary bodies formed between 1 and 2.4 AU were uniform. While another large planetary body (EPB) appears to have the same Ba, Sm, and Nd isotopic compositions as the Earth (see also Andreasen & Sharma 2006), we do not yet have precise data on the composition of the Moon and Mars. A more difficult problem is the issue of the differences in the Sm/Nd ratios of bulk planetary bodies as it is not evident that all large planets accreted with a solar Sm/Nd ratio. For example, the 18μ excess ^{142}Nd in the terrestrial upper mantle relative to ordinary chondrites and the EPB could be the result of a higher Sm/Nd ratio for bulk Earth than that of the ordinary chondrite parent bodies. For a higher Sm/Nd ratio to be the sole reason for the 18μ excess, bulk Earth would have to have a ^{147}Sm/^{144}Nd ratio that is ~5% higher than that of average chondrites. This would lead to a present day $\varepsilon_{\rm Nd}^{143}$ of bulk Earth of around +6 to +8. This value is somewhat larger than the spread in $\varepsilon_{\rm Nd}^{143}$ values of about 3 observed for chondrites.

Early differentiation of a bulk Earth with a chondritic Sm/Nd ratio, leading to an upper mantle with an average Sm/Nd ratio higher than chondritic requires sequestration of a complementary reservoir with Sm/Nd ratio lower than chondritic. Direct measurements proving the presence of the complementary reservoir have so far not been successful (Albarede 2006), but would provide unequivocal evidence for early Earth differentiation.

The enrichment factors of ^{135}Ba and ^{137}Ba for carbonaceous chondrites are about +55 ppm and are significantly different from the enrichment factors of *r*-dominant Nd and Sm isotopes that have η_r values ~0 (Fig. 3*b*). If the same *r*-process that is responsible for the Ba anomaly contributed Sm and Nd to the carbonaceous chondrites as well, we should observe a negative ^{148}Sm anomaly and positive ^{145}Nd, ^{148}Nd, and ^{150}Nd anomalies, which will be magnified by the correction for mass-dependent fractionation in the mass spectrometer source using the ^{146}Nd/^{144}Nd ratio. None of these anomalies have been observed (Andreasen & Sharma 2006). This observation requires a decoupling of the *r*-nuclei of Ba and those of Sm and Nd, and could be caused by differential adsorption of carriers of *r*-process Ba and lanthanides in the precursor material of carbonaceous chondrites. Since Ba and the lanthanides are refractory elements possibly carried by silicate phases, a differential adsorption of the carrier phases seems unlikely. If so, the observed decoupling would require that the *r*-sources of Ba are different from those of the lanthanides. That there are distinctive *r*-sources with sharp distinction in the different source contributions below and above $A \sim 140$ has been well established from (1) the observations of heavy element abundances of metal-poor stars (Burris et al. 2000; Sneden et al. 1996, 2000, 2003) and (2) extinct radionuclides ^{129}I and ^{182}Hf (Wasserburg et al. 1996). Qian et al. (1998) assigned Ba to the group of heavy *r*-nuclei and split the *r*-sources into those contributing nuclei with $A < 130$ and $A \geq 130$. Our data suggest a decoupling of *r*-process Ba from Nd and Sm and indicate that the two types of *r*-sources have to be split at $Z \leq 56$ and $Z > 56$. This is in line with the assessment of Otsuki et al. (2003).

5. CONCLUSIONS

The carbonaceous chondrites display *r*-process excesses in Ba but no corresponding anomalies in *r*-process Sm and Nd nuclides. No measurable *p*-process anomaly of Sr or Ba is observed in Allende and Murchison to a level of $\sim 1\varepsilon$ for Sr, and $\sim 1.5\varepsilon$ for Ba. This suggests different stellar sources for the Ba and lanthanide *r*-process nuclides. Great care should be taken when using one element as a proxy for another when investigating variations in nucleosynthetic contributions. Likewise, it is clear that the bulk Earth Ba, Nd, and Sm isotopic compositions cannot be estimated from carbonaceous chondrites. The ordinary chondrite and eucrite

analyzed are indistinguishable in their Sr (excluding ^{87}Sr), Ba, and Sm isotopic compositions from terrestrial standards and samples; thus, it appears reasonable to use their Nd isotopic composition as a proxy for the bulk Earth. Since the excess in ^{142}Nd $(18 \pm 8)\mu$ for the terrestrial mantle with respect to the EPB and LL-chondrite parent body cannot be related to nucleosynthetic variations, this supports the notion of early terrestrial differentiation leading to the formation, sequestration, and preservation of a reservoir with subchondritic Sm/Nd ratio on Earth. The solar nebula that fed planetesimals between ~1 and ~2.4 AU was well mixed with respect to Sr, Ba, and Sm (and Nd) isotopes. It was heterogeneous beyond ~2.7 AU where carbonaceous chondrite parent bodies formed.

We are grateful to G. J. Wasserburg for numerous discussions and insights into stellar nucleosynthesis. His critical comments on an earlier version of this manuscript guided us to make substantial improvements. E. S. Posmentier is thanked for discussions on fractionation corrections and data renormalization. Discussions with R. W. Carlson, S. B. Jacobsen, L. E. Nyquist, and R. J. Walker were very illuminating and useful. J. D. Landis is thanked for assisting with column calibrations. A thorough review by E. Zinner helped us to considerably improve this paper. Funding was provided by NSF grants EAR-0130631 and EAR-0336405, a NASA NH Space Grant, and Dartmouth College.

APPENDIX

There is a discrepancy between our Ba data and the data of Ranen & Jacobsen (2006); for large samples of Allende and Murchison we found resolvable excesses in ^{135}Ba and ^{137}Ba with respect to a terrestrial standard. In comparison, Ranen & Jacobsen (2006) found no anomalies in ^{135}Ba, but resolvable anomalies in ^{137}Ba and ^{138}Ba. Since our data appear to be consistent with other previous studies (Harper et al. 1992; Hidaka et al. 2003) and also with recently reported data on a larger set of chondrites (Carlson et al. 2007), we suggest a possible scenario that may be the cause of the observed discrepancy. Ranen & Jacobsen (2006) obtained their data in a triple-jump multidynamic collection mode, which prevented them from correcting their data for mass-dependent isotope fractionation in the ion source of the mass spectrometer using the measured isotopic ratio of the two *s*-nuclides (^{134}Ba and ^{136}Ba). Instead, they corrected their data using the measured ^{138}Ba/^{136}Ba ratio. They then renormalized their data to the ^{134}Ba/^{136}Ba ratio and observed anomalies in ^{138}Ba and ^{137}Ba, with the anomalies in ^{138}Ba/^{136}Ba being roughly twice those in ^{137}Ba/^{136}Ba.

Here we show that renormalization to the ^{134}Ba/^{136}Ba ratio for data that are already fractionation corrected using the ^{138}Ba/^{136}Ba ratio introduces a mass-dependent bias in the data and produce anomalies in ^{138}Ba that are about twice those in ^{137}Ba. This behavior is related to the uncertainty in the ^{134}Ba/^{136}Ba ratio, which is relatively large due to the low abundance of ^{134}Ba. The relationship between the original ($\varepsilon_{i,j}^{k,m}$) and renormalized ($\varepsilon_{u,v}^{k,p}$) data is given in McCulloch & Wasserburg (1978a),

$$\varepsilon_{u,v}^{k,p} = \varepsilon_{i,j}^{k,m} - \varepsilon_{i,j}^{p,m} + \left(\varepsilon_{i,j}^{v,m} - \varepsilon_{i,j}^{u,m}\right)\left(\frac{\text{mass}_k - \text{mass}_p}{\text{mass}_u - \text{mass}_v}\right),$$

where i and j are the isotopes originally used for fractionation correction, u and v are the isotopes used for renormalization, m is the original reference isotope, p is the reference isotope for the renormalized data, and k is the isotope of interest. Using synthetic data we note that this equation is exact in that it permits one to renormalize the *average* values obtained at the end of a measurement rather precisely. It is quite useful when the expected effects are relatively large (i.e., >6 σ away) compared to the external reproducibility of the isotopic ratio used for renormalization. However, if the effects are close to the order of the external reproducibility, the uncertainties associated with the measurements lead to erroneous results.

Let t, w, x, y, and z be five isotopes and T, W, and Y be deviations (usually in ε- or μ-notation) in t/x, y/x, and z/x from the standard value, when fractionation corrected to z/x. Let renormalization be done with respect to t/x and W', Y', and Z' be the renormalized deviations in w/x, y/x, and z/x from the standard value. When the same reference isotope (x) is used for renormalization, the above equation gives

$$Y' = Y - T\frac{m_y - m_x}{m_t - m_x},\ Z' = -T\frac{m_z - m_x}{m_t - m_x},\ \text{and}\ W' = W - T\frac{m_w - m_x}{m_t - m_x}.$$

We note that the presence of nonzero T values in the mass-dependent term for all the renormalized ratios will introduce mass bias into the renormalized data.

For a number of standard measurements, T, W, Y, W', Y', and Z' are defined as the deviations from the average values of that same standard population; thus, the average values are $\bar{T} = \bar{W} = \bar{Y} = \bar{W}' = \bar{Y}' = \bar{Z}' = 0$ with some estimates of analytical uncertainty associated with them. Deviations for two fractionation-corrected isotope pairs should ideally be independent (i.e., $\Delta W/\Delta Y \cong 0$). But comparing deviations for two renormalized ratios $\Delta Z'/\Delta Y'$ gives

$$\frac{\Delta Z'}{\Delta Y'} = \frac{(Z' - 0)}{(Y' - 0)} = \left(-T\frac{m_z - m_x}{m_t - m_x}\right)\Big/\left(Y - T\frac{m_y - m_x}{m_t - m_x}\right).$$

If Y and T are independent of each other this leaves a mass-dependent term $(m_z - m_x)/(m_y - m_x)$, which will lead to a mass bias in the renormalized data. This is generally the case when comparing variations in isotopes y and t, with m_y being between m_x and m_z and m_t being either lighter or heavier than m_x and m_z. If neither m_y nor m_t are between m_x and m_z, Y and T will likely not be independent, and the trend will be more complicated.

In the case of Ba, $t = ^{134}$Ba, $w = ^{135}$Ba, $x = ^{136}$Ba, $y = ^{137}$Ba, and $z = ^{138}$Ba. For Z'/Y' or ε^{138}Ba/ε^{137}Ba a slope of $(m_{138\text{Ba}} - m_{136\text{Ba}})/(m_{137\text{Ba}} - m_{136\text{Ba}})$ or ~2 is therefore expected due to the renormalization. Figure 4 plots the ε^{137}Ba and ε^{138}Ba data for 500 randomly generated standard runs and compares them with the samples and standards by Ranen & Jacobsen (2006). The synthetic data were generated in order to investigate how during data renormalization, variations in the internal precision of the ^{134}Ba/^{136}Ba ratio affect the

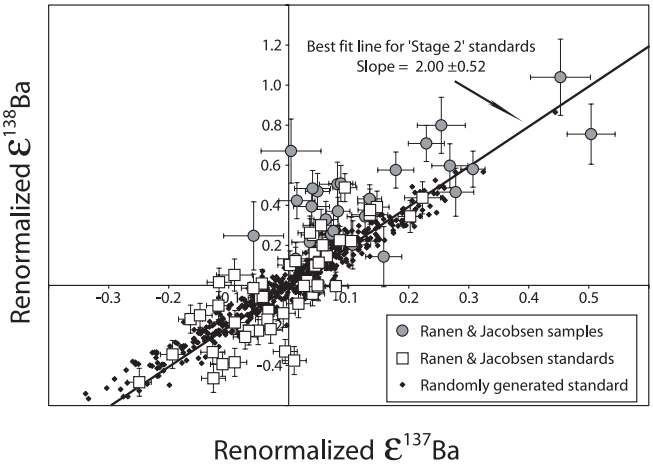

FIG. 4.—Renormalized ^{137}Ba and ^{138}Ba data reported by Ranen & Jacobsen (2006) with a best-fit line for the "stage 2" standards. Included are 500 randomly generated standard measurements based on the intensities and running time given by Ranen & Jacobsen (2006).

external reproducibility of other ratios and their mutual relationships (e.g., between ^{137}Ba/^{136}Ba and ^{138}Ba/^{136}Ba). Each of the synthetic data points is an average of 200 ratios, which were generated by assuming a ^{138}Ba ion beam of 7×10^{-11} A. Relative intensities of isotopes were determined by assuming (1) a normal Ba isotopic composition and (2) an analytical uncertainty proportional to $N^{-1/2}$, where N was calculated by integrating the ion beams for 8 s. As an end-member case we assumed that there was no mass fractionation for the duration of the synthetic measurement.

Note that the synthetically generated data (Fig. 4) define a positive slope of ~2 and plot both below and above the origin. A regression of the real standards from Ranen & Jacobsen (2006) also yields a slope of 2.0 ± 0.5 and is in excellent agreement with the randomly generated data. The external reproducibility of the ^{138}Ba/^{136}Ba ratio obtained after renormalization is *identical* to the external reproducibility of the ^{134}Ba/^{136}Ba ratio. This yields a ratio of external to internal reproducibilities for the standards to be about 4 ($=0.4\varepsilon/0.1\varepsilon$). Since this ratio converges to a value of about 1 at higher intensities, this suggests that if the data were obtained at ^{138}Ba intensities $\gg 7 \times 10^{-11}$ A, we would not be able to observe the slope, as all data would plot within error of each other. Indeed, when we plot our standards obtained at ^{138}Ba $\sim 20 \times 10^{-11}$ A (Table 2; not shown in Fig. 4 for clarity) by using the renormalization procedure, we do not find a statistically significant slope. A number of samples reported by Ranen & Jacobsen (2006) fall along the curve in Fig. 4, although there appears to be some heterogeneity. The correlated ^{137}Ba–^{138}Ba anomalies observed in the meteorite data could therefore result from the renormalization procedure. Note that the relationship is more complicated when comparing ε^{138}Ba to ε^{135}Ba (i.e., $\Delta Z'/\Delta Y'$), as both ^{134}Ba and ^{135}Ba are lighter than ^{136}Ba and ^{138}Ba used for the original fractionation correction.

Another relevant question is would the Ranen & Jacobsen (2006) data show excesses in ^{135}Ba and^{137}Ba if they were normalized initially using the ^{134}Ba/^{136}Ba ratio. The choice of Ranen & Jacobsen (2006) to correct for mass fractionation using the ^{138}Ba/^{136}Ba ratio introduces a small change in the fractionation-corrected ^{134}Ba/^{136}Ba, ^{135}Ba/^{136}Ba, and ^{137}Ba/^{136}Ba ratios for the carbonaceous chondrites due to their *r*-excess. If we correct our raw data for Allende and Murchison using the ^{138}Ba/^{136}Ba ratio we find that the ^{134}Ba/^{136}Ba ratio increases by 8 ppm, the ^{135}Ba/^{136}Ba ratio increases by 4 ppm, and the ^{137}Ba/^{136}Ba ratio decreases by 8 ppm. We note that ^{138}Ba/^{136}Ba–normalized data for Allende & Murchison from the Ranen & Jacobsen (2006) study show ^{135}Ba/^{136}Ba ratios that are slightly higher (6–40 ppm) than those reported for the terrestrial standards and ordinary chondrites. The external reproducibility for normal standards in the Ranen & Jacobsen (2006) study for ^{135}Ba/^{136}Ba is 28 ppm (2 σ standard deviation). These numbers are therefore not in conflict with the results (~39 ppm excess) reported in this study. The same argument is also valid for the ^{137}Ba excess. The Ranen & Jacobsen (2006) data fractionation corrected to ^{138}Ba/^{136}Ba show no anomalies in ^{137}Ba. With the 8 ppm lowering due to fractionation correcting to ^{138}Ba/^{136}Ba taken into account, the carbonaceous chondrites in the Ranen & Jacobsen (2006) study should show an excess of ~14 ppm. The external reproducibility for normal standards in the Ranen & Jacobsen (2006) study for ^{137}Ba/^{136}Ba is about 16 ppm (2 σ standard deviation), and their ^{137}Ba data are therefore not in conflict with the ~22 ppm excess observed in our study.

REFERENCES

Albarede, F. 2006, Nature, 444, 162
Andreasen, R., & Sharma, M. 2006, Science, 314, 806
Arlandini, C., Kappeler, F., Wisshak, K., Gallino, R., Lugaro, M., Busso, M., & Straniero, O. 1999, ApJ, 525, 886
Ashworth, J. R. 1980, Earth Planet. Sci. Lett., 46, 167
Ashworth, J. R., & Barber, D. J. 1977, Philos. Trans. R. Soc. London A, 286, 493
Becker, H., & Walker, R. J. 2003a, Nature, 425, 152
———. 2003b, Chemical Geology, 196, 43
Binzel, R. P., & Xu, S. 1993, Science, 260, 186
Birck, J. L. 2004, in Geochemistry of Non-Traditional Stable Isotopes, ed. C. M. Johnson, B. L. Beard, & F. Albarede (Washington: Mineralogical Soc. Am.), 25
Boyet, M., & Carlson, R. W. 2005, Science, 309, 576
Brandon, A. D., Walker, R. J., Puchtel, I. S. 2006, Geochim. Cosmochim. Acta, 70, 2093
Burris, D. L., Pilachowski, C. A., Armandroff, T. E., Sneden, C., Cowan, J. J., & Roe, H. 2000, ApJ, 544, 302
Carlson, R. W., Boyet, M., & Horan, M. F. 2007, Science, 316, 1175
Chabaux, F., Benothman, D., & Birck, J. L. 1994, Chem. Geo., 114, 191
Chambers, J. E. 2004, Earth Planet. Sci. Lett., 223, 241
Chen, J. H., Papanastassiou, D. A., & Wasserburg, G. J. 1998, Geochim. Cosmochim. Acta, 62, 3379
Clayton, D. D., Amari, S., & Zinner, E. 1997, Ap&SS, 251, 355
Consolmagno, G. J., & Drake, M. J. 1977, Geochim. Cosmochim. Acta, 41, 1271
Eugster, O., Tera, F., & Wasserburg, G. J. 1969, J. Geophys. Res., 74, 3897
Fujii, T., Moynier, F., & Albarede, F. 2006, Earth Planet. Sci. Lett., 247, 1
Glavin, D. P., & Lugmair, G. W. 2003, Lunar Planet. Sci. Conf., 34, 1276
Harper, C. L., Weismann, H., & Nyquist, L. E. 1992, Meteoritics, 27, 230
Hayakawa, T., Iwamoto, N., Shizuma, T., Kajino, T., Umeda, H., & Nomoto, K. 2005, Nucl. Phys. A, 758, 525

Hidaka, H., Ohta, Y., & Yoneda, S. 2003, Earth Planet. Sci. Lett., 214, 455
Hidaka, H., Ohta, Y., Yoneda, S., & DeLaeter, J. R. 2001, Earth Planet. Sci. Lett., 193, 459
Huss, G. R. 1990, Nature, 347, 159
Huss, G. R., & Lewis, R. S. 1995, Geochim. Cosmochim. Acta, 59, 115
Jennings, C. L., Savina, M. R., Messenger, S., Amari, S., Nichols, R. H. J., Pellin, M. J., & Podosek, F. A. 2002, Lunar Planet. Sci. Conf., 33, 1833
Lee, T., Papanastassiou, D. A., & Wasserburg, G. J. 1978, ApJ, 220, L21
Leroux, H., Doukhan, J., & Guyot, F. 1996, Meteoritics Plan Sci., 31, 767
Lewis, R. S., Anders, E., Shimamura, T., & Lugmair, G. W. 1983, Science, 222, 1013
Lewis, R. S., Huss, G. R., & Lugmair, G. W. 1991, Lunar Planet. Sci. Conf., 22, 807
Lodders, K., & Amari, S. 2005, Chem. Erde-Geochem., 65, 93
Lugaro, M., Davis, A. M., Gallino, R., Pellin, M. J., Straniero, O., & Kappeler, F. 2003, ApJ, 593, 486
Lugmair, G. W., Marti, K., & Scheinin, N. B. 1978, Lunar Planet. Sci. Conf., 9, 672
Lugmair, G. W., Shimamura, T., Lewis, R. S., & Anders, E. 1983, Science, 222, 1015
Mathews, G. J., & Fowler, W. A. 1981, ApJ, 251, L45
McCulloch, M. T., & Wasserburg, G. J. 1978a, ApJ, 220, L15
———. 1978b, Geophys. Res. Lett., 5, 599
Messenger, S., Keller, L. P., & Lauretta, D. S. 2005, Science, 309, 737
Meyer, B. S., & Zinner, E. 2006, in Meteorites and the Early Solar System II, ed. D. S. Lauretta & H. Y. J. McSween (Tucson: Univ. Arizona Press), 69
Nakamura, N. 1974, Geochim. Cosmochim. Acta, 38, 757
Nichols, R. H. J., Brannon, J. C., & Podosek, F. A. 2002, Lunar Planet. Sci. Conf., 33, 1929
Niederer, F. R., Papanastassiou, D. A., & Wasserburg, G. J. 1981, Geochim. Cosmochim. Acta, 45, 1017
Nittler, L. R. 2003, Earth Planet. Sci. Lett., 209, 259
O'Brien, D. P., Morbidelli, A., & Levison, H. F. 2006, Icarus, 184, 39
Otsuki, K., Mathews, G. J., & Kajino, T. 2003, NewA, 8, 767
Ott, U., & Begemann, F. 1990, ApJ, 353, L57
Papanastassiou, D. A., & Wasserburg, G. J. 1978, Geophys. Res. Lett., 5, 595
Patchett, P. J. 1980, Earth Planet. Sci. Lett., 50, 181
Pilger, C., Leis, F., Tschopel, P., Broekaert, J. A. C., & Tolg, G. 1995, Fresenius J. Anal. Chem., 351, 110
Podosek, F. A., Prombo, C. A., Amari, S., & Lewis, R. S. 2004, ApJ, 605, 960
Prombo, C. A., Podosek, F. A., Amari, S., & Lewis, R. S. 1992, Lunar Planet. Sci. Conf., 23, 1111
———. 1993, ApJ, 410, 393
Qian, Y. Z., Vogel, P., & Wasserburg, G. J. 1998, ApJ, 494, 285
Ranen, M. C., & Jacobsen, S. B. 2006, Science, 314, 809
Rankenburg, K., Brandon, A. D., & Neal, C. R. 2006, Science, 312, 1369
Russell, W. A., Papanastassiou, D. A., & Tombrello, T. A. 1978, Geochim. Cosmochim. Acta, 42, 1075
Savina, M. R., et al. 2003, Geochim. Cosmochim. Acta, 67, 3201
Schönbächler, M., Lee, D. C., Rehkämper, M., Halliday, A. N., Fehr, M. A., Hattendorf, B., & Gunther, D. 2003, Earth Planet. Sci. Lett., 216, 467
Sneden, C., Cowan, J. J., Ivans, I. I., Fuller, G. M., Burles, S., Beers, T. C., & Lawler, J. E. 2000, ApJ, 533, L139
Sneden, C., McWilliam, A., Preston, G. W., Cowan, J. J., Burris, D. L., & Armosky, B. J. 1996, ApJ, 467, 819
Sneden, C., et al. 2003, ApJ, 591, 936
Tizard, J., Lyon, I., & Henkel, T. 2005, Meteoritics Planet. Sci., 40, 335
Virag, A., Wopenka, B., Amari, S., Zinner, E., Anders, E., & Lewis, R. S. 1992, Geochim.Cosmochim. Acta, 56, 1715
Wasserburg, G. J., Busso, M., & Gallino, R. 1996, ApJ, 466, L109
Wasserburg, G. J., Papanastassiou, D. A., & Lee, T. 1980, in Early Solar System Processes and The Present Solar System, ed. P. Papali (Bologna: Societa Italiana di Fisica), 144
Wolf, S. F., Unger, D. L., & Friedrich, J. M. 2005, Analytica Chim. Acta, 528, 121
Yin, Q. Z., Lee, C. T. A., & Ott, U. 2006, ApJ, 647, 676
Yokoyama, T., et al. 2007, Lunar Planet. Sci. Conf., 38, 1151
Zinner, E. 1998, Annu. Rev. Earth Planet. Sci., 26, 147
Zinner, E., Amari, S., & Lewis, R. S. 1991, ApJ, 382, L47